Extended target PMBM tracker with a Gaussian Process target model on LiDAR data

1st Martin Baerveldt
Dept. of Engineering Cybernetics
NTNU
Trondheim, Norway
martin.baerveldt@ntnu.no

2nd Michael Ernesto López
Dept. of Engineering Cybernetics
NTNU
Trondheim, Norway
ernesto.lopez@ntnu.no

3rd Edmund Førland Brekke
Dept. of Engineering Cybernetics
NTNU
Trondheim, Norway
edmund.brekke@ntnu.no

***Abstract*—In Multiple Extended Object Tracking, the PMBM (Poisson Multi-Bernoulli Mixture) tracker is considered state-of-the-art. Originally, it was presented with the GGIW (Gamma Gaussian Inverse Wishart) target model, which is a random matrix model. When tracking larger objects using LiDAR, measurements are generated by the contour rather than the whole target surface, and it is beneficial to model this with the target model. A target model which has this capability is the Gaussian Process (GP) extent model. This paper presents a PMBM tracker using this target model. We also discuss considerations related to the use of the GP model in the PMBM framework. Secondly, we present improvements in the target model which increases the robustness of the model by dealing with the inherent non-linearities using the Gauss-Newton method. We also present a comparison with the GGIW-PMBM tracker on simulated and real LiDAR data gathered from maritime vessels.**

***Index Terms*—Multi-target tracking, Bayesian estimation, Extended Targets, Gaussian Processes**

I. Introduction

Target tracking, the issue of estimating the kinematic state of one or several objects, has long used the point-approximation when parsing sensor data. With the advent of high-resolution sensors, it is now common that a measurement source gives rise to multiple measurements. This has given rise to extended target tracking models which enables the modeling of a target's extent in addition to its kinematic properties [1]. Initial approaches used an elliptic shape as prior [2]. This is known as the random matrix model. A version of this model, the GGIW model, was used to demonstrate an Extended Target PMBM filter [3] which builds on the original PMBM filter [4]. This filter has been expanded on with several improvements with regards to data association and merging [5]–[8], as well as a tracker using the sets of trajectories framework [9]. The random matrix model is not the only target model for extended targets though. Another approach models the extent using star-convex shapes and represents the shape using a parametrization of the contour [10]. This enables the modeling of more complex shapes. It also allows an easier way to model measurements that originate from the contour, such as measurements generated by a LiDAR. The most promising and investigated of these models uses Gaussian Processes to estimate the extent [11]. This model has been used in another Multi-target tracking filter, the δ-GLMB filter [12]. In previous work comparing different filter structures it has been shown that the PMBM has a more efficient structure and it can initialize a track faster with its Poisson birth model as compared to Bernoulli birth models [13]. In this paper, we aim to present an Extended Target PMBM tracker using the Gaussian Process target model and provide an example of a Poisson birth density. We present the applicable prediction and update formulas. We also introduce an improvement to dealing with the nonlinearity of the measurement model for the Gaussian Process method, which has previously been explored in [14]–[16]. Finally, we show the application of the developed tracker on LiDAR data gathered by tracking smaller maritime vessels.

The research leading to these results has received funding from the European Union's Horizon 2020 research and innovation programme under the Marie Skłodowska-Curie grant agreement No 955.768 (MSCA-ETN AUTOBarge). This publication reflects only the authors' view, exempting the European Union from any liability. Project website: http://etn-autobarge.eu/. This work was supported in part by the Research Council of Norway through Projects 295033 and 309230.

II. Background

Below we present a summary of the method of extent estimation using Gaussian Processes presented in [11]. Then we outline the theory related to the PMBM filter which was presented in [3] and the extension of the theory to sets of trajectories which was presented in [9].

A. Gaussian Process

A Gaussian process (GP) can be considered a distribution over functions [17]. It is completely specified by its mean function $m(\gamma)$ and covariance function $k(\gamma, \gamma')$. Using Gaussian processes to estimate a radial function means that we can write

$$f(\theta) \sim \mathcal{GP}(m(\theta), k(\theta, \theta')) \tag{1}$$

Where $f(\theta)$ defines the radius at angle θ. We want to estimate the values of this function using measurements of only some of its values. This is a method known as GP regression. We define a vector of N different points known as test points $\Theta^f = [\theta_1^f \quad ... \quad \theta_N^f]$. Further, we define a measurement model as

$$z_k = f(\theta_k) + \eta_k, \quad \eta \sim \mathcal{N}(0, R) \tag{2}$$

Where z_k is the measurement, θ_k is the training input which is the point at which the measurements are taken and η_k is the measurement noise. If we have m measurements of the function we define $\mathbf{z} = [z^1 \quad ... \quad z^m]$ and their corresponding input values $\Theta = [\theta_1 \quad ... \quad \theta_m]$ to learn the function values for $\mathbf{\Theta^f}$. In the original paper [11], it is shown that the state $\mathbf{x}^f = \left[f(\theta_1^f)...f(\theta_N^f)\right]^T$, which defines the extent, can be recursively estimated using the following state space model

$$\begin{aligned} \mathbf{x}_{k+1}^f &= F^{\mathbf{f}}\mathbf{x^f}_k + \mathbf{w}_k, \quad \mathbf{w}_k \sim \mathcal{N}(0, Q^{\mathbf{f}}) \\ z_k &= H^f(\theta_k)\mathbf{x}_k^f + \epsilon_k^f, \quad \epsilon_k^f \sim \mathcal{N}(0, R^f) \end{aligned} \tag{3}$$

where the measurement model is given by

$$\begin{aligned} H^f(\theta_k) &= K(\theta_k, \Theta^f)\left[K(\Theta^f, \Theta^f)\right]^{-1} \\ R^f(\theta_k) &= k(\theta_k, \theta_k) + R - H^f(\theta_k)K(\Theta^f, \theta_k) \end{aligned} \tag{4}$$

where K in turn is defined as a covariance matrix where the elements are made up of the elementwise evaluation of the covariance function $k(\gamma, \gamma')$. The process model is defined by

$$F^{\mathbf{f}} = e^{-\alpha T}I, \quad Q^{\mathbf{f}} = \left(1 - e^{-2\alpha T}\right)K(\Theta^f, \Theta^f) \tag{5}$$

The parameter for this model is a forgetting factor α.

1) Covariance functions: If, as is commonly done, the GP is defined with zero mean, the covariance function is the component that defines the GP and any prior information about the shapes. Therefore, we want to encode the periodicity of $f(\theta)$ in the covariance function. Such a function was presented in the original paper and it was defined with three parameters, σ_f, σ_r, and l.

It is also desirable to design a covariance function that encodes axial symmetry since in many cases targets are symmetric about the longitudinal axis. Since the longitudinal axis is defined at $\theta = 0$ this is equivalent to an even function. One such function can be built using the smallest signed angle function

$$ssa(\theta) \coloneqq \pi - [(\pi - \theta)(\mod 2\pi)] \tag{6}$$

i.e. $ssa(\theta)$ is the only angle in $(-\pi, \pi]$ such that $ssa(\theta) \equiv \theta$. The absolute value of this function is both 2π-periodic and even which is the property we sought. We define the symmetric covariance function as

$$k(\theta, \theta') = \sigma_f^2 e^{-\frac{1}{2l^2}(|ssa(\theta)| - ssa|\theta'|)^2} + \sigma_r^2 + \sigma_n^2\delta(\theta, \theta') \tag{7}$$

σ_n is another noise term added that makes it easier to model sharp edges by adding a small term to each diagonal part of the constructed covariance matrix. This has the added benefit of regularizing the covariance matrix [18].

B. State space model for extended targets

To perform joint estimation of the extent and state of the target an augmented state space vector is defined

$$\mathbf{x}_k = \begin{bmatrix}\mathbf{x}_k^c & \phi_k & (\mathbf{x}_k^*) & \mathbf{x}_k^{\mathbf{f}}\end{bmatrix}^T \tag{8}$$

Where $\mathbf{x}_k^c$ is the position of the centroid of the target from which the extent is defined, ϕ is the heading of the target and $\mathbf{x}_k^*$ are any additional kinematic states of the target. In the original paper, these are the velocity in each direction in 2D and the angular velocity $\dot{\phi}$. We use the same state space vector in this paper.

For this augmented state space vector we define the following state space description

$$\begin{aligned} \mathbf{x}_{k+1} &= F\mathbf{x}_k + \mathbf{w}, \quad \mathbf{w} \sim \mathcal{N}(0, Q) \\ \mathbf{z}_k &= \mathbf{h}_k(\mathbf{x}_k) + \eta_k, \quad \epsilon_k \sim \mathcal{N}(0, R_k) \end{aligned} \tag{9}$$

Where $\mathbf{z_k}$, $\mathbf{h}_k(\mathbf{x}_k)$ and R_k are all augmentations given by measurements of one scan of the target.

The random hypersurface model defines a measurement equation for a target contour parametrized by a function f.

$$\begin{aligned} z_k^l &= \mathbf{x}_k^c + \mathbf{p}(\theta_k^l)f(\theta_k^l) + \eta_k^l \\ \mathbf{p}(\theta_k^l) &= \begin{bmatrix}\cos\theta_k^l \\ \sin\theta_k^l\end{bmatrix} \end{aligned} \tag{10}$$

Where z_k^l is the measurement l at time k and θ_k^l is the corresponding angle of the origin of the measurement of the target contour. θ_k^l can be expressed both in a global frame ${\theta_k^l}^{(G)}$ and the local target frame ${\theta_k^l}^{(L)}$ as

$$\begin{aligned} {\theta_k^l}^{(L)}(\mathbf{x}_k^c, \phi_k) &= {\theta_k^l}^{(G)}(\mathbf{x}_k^c) - \phi_k \\ {\theta_k^l}^{(G)}(\mathbf{x}_k^c) &= \angle(\mathbf{z}_{k,l} - \mathbf{x}_k^c) \end{aligned} \tag{11}$$

Plugging the expressions for GP regression (3) into the measurement equation (10) we attain

$$\begin{aligned} \mathbf{z}_k^l &= \mathbf{x}_k^c + \mathbf{p}_k^l({\theta_k^l}^{(G)}(\mathbf{x}_k^c))H^{\mathbf{f}}\left({\theta_k^l}^{(L)}(\mathbf{x}_k^c, \phi_k)\right)\mathbf{x}_k^f + \eta_k^l \\ &= h_k^l(\mathbf{x}_k) + \eta_k^l, \qquad \eta_k^l \sim \mathcal{N}(0, R_k^l) \\ R_k^l &= \mathbf{p}_k^l(\mathbf{x}_k^c)R^f\left({\theta_k^l}^{(L)}(\mathbf{x}_k^c, \phi_k)\right)\mathbf{p}_k^l(\mathbf{x}_k^c)^T + R \end{aligned} \tag{12}$$

This is a non-linear measurement model and therefore needs to be estimated using a non-linear filtering technique. It should be noted that this is an implicit equation due to the dependence of $\mathbf{z}_k^l$ contained in ${\theta_k^l}^{(G)}(\mathbf{x}_k^c)$.

For the motion model, the motion can be described with a linear state space model and this can be combined with the process model for the extent as

$$F = \begin{bmatrix}\bar{F} & 0 \\ 0 & F^{\mathbf{f}}\end{bmatrix}, Q = \begin{bmatrix}\bar{Q} & 0 \\ 0 & Q^{\mathbf{f}}\end{bmatrix} \tag{13}$$

Where $F^{\mathbf{f}}$ and $Q^{\mathbf{f}}$ are given by equation (5) and $\bar{F}$ and $\bar{Q}$ are given by the motion model used. For this work, we use the constant velocity model with constant turn where we define

$$\begin{aligned} \bar{F} &= \begin{bmatrix}1 & dt \\ 0 & 1\end{bmatrix} \otimes I_3, \\ \bar{Q} &= \begin{bmatrix}\frac{dt^3}{3} & \frac{dt^2}{2} \\ \frac{dt^2}{2} & dt\end{bmatrix} \otimes \begin{bmatrix}\sigma_c^2 & 0 & 0 \\ 0 & \sigma_c^2 & 0 \\ 0 & 0 & \sigma_\phi^2\end{bmatrix} \end{aligned} \tag{14}$$

where dt is the sampling time and σ_c is the process noise variance for position and σ_ϕ is the process noise variance for the heading angle.

C. The PMBM filter

To model the problem of tracking multiple targets, the PMBM filter utilizes Random Finite Sets (RFS) to model both the unknown number of targets and the unknown number of measurements. The set of object states at time k is modeled as $X_k = \{x_k^1, \cdots, x_k^{n_k}\}$ and the measurements collected at time step k are defined as $Z_k = \{z_k^1, \cdots, z_k^{m_k}\}$ with z_k^i denoting a single measurement.

The PMBM conjugate prior is a combination of a PPP (Poisson Point Process) and an MBM (Multi-Bernoulli Mixture), where the PPP represents the targets that have not been detected $\mathbf{X}_k^u$ and the MBM represents the targets that have been detected $\mathbf{X}_k^d$. A PMBM density is fully parametrized by

$$D_k^u, \{w_k^j, \{r_k^{j,i}, (f_k^{j,i})\}_{i\in\mathbb{T}_{k|k'}}\}_{j\in\mathbb{J}_{k|k'}} \tag{15}$$

where D_k^u is the intensity of the PPP for the unknown targets. The Bernoulli modeling target i is represented by the probability density $f_k^{j,i}$ which represents both the kinematic state and the extent of the target, along with any additional information that can be inferred from it. A Bernoulli set also contains a parameter r, representing a target's existence probability. The different components in the Multi-Bernoulli Mixture are represented by an index $j \in \mathbb{J}$ and correspond to a data association hypothesis with the weight w^j representing the relative likelihood of each hypothesis. Additional assumptions are that new targets appear in the region according to a PPP with birth intensity D_k^b, targets survive with probability P^S and evolve with a transition density $\mathbf{g}_{k|k-1}$. Clutter is modeled as a PPP with rate λ_c. Each target is detected with a probability P^D and if detected, generates measurements according to a PPP with rate $\lambda_m(\mathbf{x}_k)$ and a spatial distribution $l(Z_C|\mathbf{x}_k)$, given by the chosen target model. Z_C is the subset of measurements assigned to a specific measurement cell C, and l_C is the likelihood of this assignment. Recursions based on these assumptions are presented in the original paper on the PMBM filter for extended objects [3]. It has also been extended to a full tracker by using sets of trajectories [9].

D. Estimating measurement rate

The Poisson rate $\lambda^m(\mathbf{x})$ represents the cardinality of the measurement set, i.e., the expected number of measurements. One assumption is a constant rate but this is not in good agreement with the physical reality of many sensors since the number of returns scales by distance. One approach was developed in [19] and has since been used as part of the GGIW target model in several works such as [3], [20]. It has also been used in combination with the Gaussian Process model [12]. It utilizes that a Poisson rate can be estimated using a gamma distribution due to it being the conjugate prior for the Poisson distribution. A gamma distribution can be parametrized by parameters α and β, where α is the shape parameter and β is the inverse scale parameter, i.e. $\lambda^m \sim \mathcal{G}(\alpha, \beta)$. These can be updated using the following recursions

$$\begin{aligned} \alpha_{k|k-1} &= \frac{\alpha_{k-1}}{\eta_\gamma}, \qquad \beta_{k|k-1} = \frac{\beta_{k-1}}{\eta_\gamma} \\ \alpha_k &= \alpha_{k|k-1} + |Z_C|, \qquad \beta_k = \beta_{k|k-1} + 1 \end{aligned} \tag{16}$$

The forgetting factor η_γ is defined by $\eta_\gamma = \frac{1}{1-w_e}$, which means that only information from the time steps within the window length is trusted. These parameters are also incorporated into the state vector for each target.

III. GP Implementation

Given the state space model presented above, we now provide the specific closed-form expression for the PMBM filter recursions for this model. We then discuss specific considerations for using the GP model in the PMBM framework and present the approximations used to make the tracker computationally feasible. We use the same notation as [3] for the derivations.

A. PMBM Filter Recursions with a GP target model

For the special case where the probability of survival P^S is constant and the following holds

$$\begin{aligned} D_{k-1}^u(\mathbf{x}) &= \sum_{n=1}^{N_u} d_n^u \mathcal{N}(\mathbf{x}; \mathbf{x}_n^u, \mathbf{P}_n^u)\mathcal{G}(\alpha_n^u, \beta_n^u) \\ f_{k-1}^{j,i}(\mathbf{x}) &= \mathcal{N}(\mathbf{x}; \mathbf{x}_{k-1}^{j,i}, \mathbf{P}_{k-1})\mathcal{G}(\alpha_{k-1}^{j,i}, \beta_{k-1}^{j,i}) \\ \mathbf{g}_{k|k-1}(\mathbf{x}|\mathbf{x}') &= \mathcal{N}(\mathbf{x}; \mathbf{F}\mathbf{x}', \mathbf{Q}) \end{aligned} \tag{17}$$

i.e., the probability distribution representing the target state in the Bernoulli components is a gamma-gaussian distribution and the PPP intensity is a linear combination of gamma-gaussian distributions, i.e., a gamma-Gaussian mixture. The state transition density for the gaussian and the gamma component is assumed to be independent, which enables separate prediction of the state and extent from the measurement rate. This assumption was used in [19]. The closed-form expression is then given by

$$\begin{aligned} D_{k|k-1}^u(\mathbf{x}) &= D^b(\mathbf{x}) \\ &\quad + P^S \sum_{n=1}^{N_u} d_n^u \mathcal{N}(\mathbf{x}; \mathbf{F}\mathbf{x}_n^u, \mathbf{F}\mathbf{P}_n^u\mathbf{F}^T + \mathbf{Q})\mathcal{G}(\alpha_n^u, \beta_n^u) \\ w_{k|k-1}^j &= w_k^j \\ r_{k|k-1}^{j,i} &= r_k^{j,i} P^S \\ f_{k|k-1}^{j,i} &= \mathcal{N}(\mathbf{x}; \mathbf{F}\mathbf{x}_{k-1}^{j,i}, \mathbf{F}\mathbf{P}_{k-1}^{j,i}\mathbf{F}^T + \mathbf{Q})\mathcal{G}(\alpha_{k|k-1}^{j,i}, \beta_{k|k-1}^{j,i}) \end{aligned} \tag{18}$$

For the update step, we define the following assumption regarding the single measurement likelihood

$$l(z|\mathbf{x}) \approx \mathcal{N}(z; h(\mathbf{x}), \mathbf{R}) \approx \mathcal{N}(z; \mathbf{H}_k, \mathbf{R_k}) \tag{19}$$

i.e. $h(\mathbf{x})$ defined in (12) is approximated by its jacobian $\mathbf{H}_k$. We further define the following

$$\begin{aligned} f_{k|k-1}^{j,i}(\mathbf{x}) &= \mathcal{N}(\mathbf{x}; \mathbf{x}_{k|k-1}^{j,i}, \mathbf{P}_{k|k-1}^{j,i})\mathcal{G}(\alpha_{k|k-1}^{j,i}, \beta_{k|k-1}^{j,i}) \\ D_{k|k-1}^u(\mathbf{x}) &= \sum_{n=1}^{N_u} d_n^u \mathcal{N}(\mathbf{x}; \mathbf{x}_n^u, \mathbf{P}_n^u)\mathcal{G}(\alpha_n^u, \beta_n^u) \\ l_C(\alpha, \beta, \mathbf{x}, \mathbf{P}, Z_C) &= \frac{\Gamma(\alpha + |Z_C|)\beta^\alpha}{\Gamma(\alpha)(\beta+1)^{(\alpha+|Z_C|)}|Z_C|!} \\ &\quad \times \prod_{z\in Z_C} \mathcal{N}(z; \bar{\mathbf{z}}, \mathbf{S}_k) \end{aligned} \tag{20}$$

where l_C is defined as the predicted likelihood of measurement cell C, the parameters $\bar{\mathbf{z}}$ and $\mathbf{S}_k$ are given by a Kalman Filter update step and are as such defined by the matrices $\mathbf{H}_k$, $\mathbf{R}_k$ and $\mathbf{P}_k$ and the prior target state $\mathbf{x}_k$ of the target corresponding to the measurement cell. It is again assumed that the measurement rate and the combined state and extent are independent. The predicted likelihood of the gamma component was derived in [19].

If we further assume that the probability of detection P^D is constant then we can derive the following closed-form expressions. The PPP component representing undetected targets is updated as

$$D_k^u(\mathbf{x}) = Q^D D_{k|k-1}^u(\mathbf{x}) \tag{21}$$

I.e. the weight of each undetected target in the mixture is updated with the probability of misdetection, defined as

$$Q^D = 1 - P^D \tag{22}$$

The MBM is updated based on the associations made of measurements to measurement cells. The weights for the association hypotheses are updated as

$$w_k^{j,A} = \frac{w_{k|k-1}^j \prod_{C \in A} L^{j,C}}{\sum_{j \in \mathbb{J}_{k|k-1}} \sum_{A \in \mathcal{A}_j} w_{k|k-1}^j \prod_{C \in A} L^{j,C}} \tag{23}$$

i.e. the weight of an association hypothesis A is given by a product of the likelihoods L of all measurement cells, normalized over all association hypotheses.

The updated parameters for the gaussian distributions are given by a Kalman filter update step and the updated gamma parameters for a measurement cell are given by (16).

The form of the update step for measurement cell C depends on if the measurement cell is associated with a detected or undetected target. The current time index k is omitted for brevity. For detected targets, we have two cases to consider

$$\begin{aligned}
L^{j,C} &= \begin{cases} 1 - r_{k|k-1}^{j,i_C} + r_{k|k-1}^{j,i_C} Q^D & |Z_C| = 0 \\ r_{k|k-1}^{j,i_C} P^D l_C(\alpha^{j,i}, \beta^{j,i}, \mathbf{x}^{j,i}, \mathbf{P}^{j,i}, Z_C) & |Z_C| \neq 0 \end{cases} \\
r_k^{j,C} &= \begin{cases} \frac{r_{k|k-1}^{j,i_C} Q^D}{1 - r_{k|k-1}^{j,i_C} + r_{k|k-1}^{j,i_C} Q^D} & |Z_C| = 0 \\ 1 & |Z_C| \neq 0 \end{cases} \\
f_k^{j,C}(\mathbf{x}) &= \begin{cases} \mathcal{N}(\mathbf{x}; \mathbf{x}_{k|k-1}^{j,i_C}, \mathbf{P}_{k|k-1}^{j,i_C}) \mathcal{G}(\alpha^{j,i_C}, \beta^{j,i_C}) & |Z_C| = 0 \\ \mathcal{N}(\mathbf{x}; \hat{\mathbf{x}}^{j,i_C}, \hat{\mathbf{P}}^{j,i_C}) \mathcal{G}(\alpha^{j,i_C}, \beta^{j,i_C}) & |Z_C| \neq 0 \end{cases}
\end{aligned} \tag{24}$$

If measurements are assigned to undetected targets, there are also two cases to consider, since it is assumed that a cell containing more than one measurement cannot be clutter-originated. Note that the result is a component of the MBM since the target has now been detected.

$$\begin{aligned}
L^{j,C} &= \begin{cases} D^c + P^D \sum_{n=1}^{N^u} d_n^u l_C(\alpha_n^u, \beta_n^u, \mathbf{x}_n^u, \mathbf{P}_n^u, Z_C) & |Z_C| = 1 \\ P^D \sum_{n=1}^{N^u} d_n^u l_C(\alpha_n^u, \beta_n^u, \mathbf{x}_n^u, \mathbf{P}_n^u, Z_C) & |Z_C| > 1 \end{cases} \\
r_k^{j,C} &= \begin{cases} \frac{P^D \sum_{n=1}^{N^u} d_n^u l_C(\alpha_n^u, \beta_n^u, Z_C, \mathbf{x}_n^u, \mathbf{P}_n^u)}{D^c + P^D \sum_{n=1}^{N^u} d_n^u l_C(\alpha_n^u, \beta_n^u, Z_C, \mathbf{x}_n^u, \mathbf{P}_n^u)} & |Z_C| = 1 \\ 1 & |Z_C| > 1 \end{cases} \\
f_k^{j,C}(\mathbf{x}) &= \sum_{n=1}^{N^u} d_n^u \mathcal{N}(\mathbf{x}; \hat{\mathbf{x}}_n^u, \hat{\mathbf{P}}_n^u) \mathcal{G}(\alpha_n^u, \beta_n^u)
\end{aligned} \tag{25}$$

B. Handling nonlinearities in the measurement equation

Since the measurement equation (12) is nonlinear there arises a need to use non-linear filtering to deal with this non-linearity and estimate $\mathbf{H}$. The original paper on the GP model simply applies the Extended Kalman Filter [11]. Subsequent work has been done to improve this method by dealing with the nonlinearities differently or augmenting the approach [14]–[16]. We propose using the iterated Extended Kalman Filter (IEKF) to improve the linearization. It has been shown that applying the IEKF is equivalent to Gauss-Newton (GN) Optimization of the maximum likelihood function defined as

$$q(\xi) = \left(\begin{bmatrix} \mathbf{z}_k \\ \hat{\mathbf{x}} \end{bmatrix} - \begin{bmatrix} \mathbf{h}(\xi) \\ \xi \end{bmatrix} \right) \begin{bmatrix} \mathbf{R} & 0 \\ 0 & \mathbf{P} \end{bmatrix}^{-1} \left(\begin{bmatrix} \mathbf{z}_k \\ \hat{\mathbf{x}} \end{bmatrix} - \begin{bmatrix} \mathbf{h}(\xi) \\ \xi \end{bmatrix} \right) \tag{26}$$

Where $\mathbf{h}(\xi)$ and $\mathbf{z}_k$ are defined by (9) and (12). It is therefore Maximum a Posteriori estimator of the state [21]. Equivalently the IEKF will suffer from the same shortcomings as Gauss-Newton methods, in particular when there are several local optima or the initialization point is far away. In this specific case, $\mathbf{h}(x)$ is not globally convex and has several local optima.

To mitigate this, we suggest designing a set of heuristic constraints for the initial point of the optimization to ensure that it converges on the most relevant local optimum. In [15], the concept of negative information is used to augment the model. Inspired by this, we can define constraints for the centroid $\mathbf{x}^c$. Consider a return from a laser ranging sensor hitting an extended object. We can then state the following constraint for $\mathbf{x}^c \coloneqq (x^p, y^p)$ given more than two measurements

$$\begin{aligned}
\alpha_{min} < atan2(\frac{y^p}{x^p}) < \alpha_{max} \\
\min r_z < \sqrt{(y^p)^2 + (x^p)^2}
\end{aligned} \tag{27}$$

Where $\alpha_{min/max}$ is the maximum and minimum angle of all measurements and $\min r_z$ is the radial distance of the measurement closest to the sensor. I.e., the center of the extended object's angle with regards to the sensor should be between the minimum and maximum angle, and it should be further away than the closest measurement return. Enforcing this condition prior to optimization by setting x^c according to

$$\begin{aligned}
\mathbf{x}^c &= \text{pol2cart}(\alpha_{max/min}, ||\mathbf{x}^c||) \\
\mathbf{x}^c &= \text{pol2cart}(\angle \mathbf{x}^c, \min r_z + \min \mathbf{x}^f)
\end{aligned} \tag{28}$$

means that $\mathbf{x}^c$ will be initiated behind the sensor wall.

Another issue is that this model is generally not observable, especially with few measurements. Therefore there is no unique solution and the solution depends on the choice of prior used to initialize the estimate. Therefore, the choice of prior is of key importance. Particularly the general characteristics of the extent prior as well as the prior value of the heading need to be specified.

C. Initialization and birth process

In the PMBM framework, the prior estimates are encoded in birth process intensity D_b. By using the mixture representation of the PPP intensity function, i.e.

$$D(\mathbf{x}) = \sum_{i \in \mathrm{I}} w_b^i p_b^i(\mathbf{x}) \tag{29}$$

we can define several priors and since the weight of the PPP components will be updated based on the likelihood of the measurements, the resulting estimate will be weighted. Selecting these priors is still not a trivial choice and in most cases are tuned to fit the particular problem. For instance, in [12] where a gaussian process model was used to track vehicles, the prior for the extent (i.e. $\mathbf{x}_0^{\mathbf{f}}$) was chosen to correspond to the extent of a real vehicle. In this work, we assume an expected maximum range of the sensor and use it to set the positional component of the birth process. I.e., spread the mixture components uniformly beyond the edge of the circle defined by the maximum range of the sensor. By placing it beyond, the centroid will be placed behind the first measurements. The heading can be defined by the direction toward the sensor and the direction of the velocity vector can be defined similarly. The magnitude of the vector should be tuned to the expected velocity of the targets. The angular velocity can be assumed to be 0 rad/s. The covariance of all these kinematic states is inflated to ensure that the mixture components can represent a variety of states. With regards to the extent, it should be tailored to the targets that are expected to appear. In this case, because we are tracking ships, we define the extent prior as a ship-like shape with a pointed bow and a flat stern with symmetry along the vertical axis. If it is desirable to track targets with very different shapes, one can also include different shapes in the birth intensity function.

D. Mixture Reduction

Mixture reduction is also a necessary tool used in the birth process to reduce all the components in the PPP component into one Bernoulli. It can also be used to merge Bernoullis that are similar. The merging is done using standard Gaussian mixture reduction for the kinematic and extent states and by the method derived in [19] for the parameters of the gamma distribution.

E. Reducing Associations

To reduce the number of data associations, gating is performed as an initial step. Gating for the GP model was presented in the original paper and the same method is used in this work [11]. This separates the targets and measurements into independent subgroups. Further reduction of association hypotheses is done using the stochastic optimization method presented in [5] to find the most likely associations.

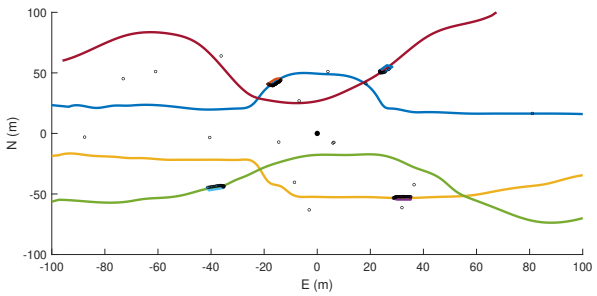

Fig. 1. Visualization of the simulation scenario, along with the extent and measurements visualized for a single timestep

IV. Simulation Study

In this section, we present the result from a Monte Carlo simulation study where the performance of the PMBM-tracker using the presented GP model is compared with the implementation using the GGIW model as presented in [9] [1].

A. Simulation Scenario

The scenario consists of 4 ships approaching from the edge of the surveillance area and traversing it to the opposite end including a turning maneuver. See Fig 1 for a detailed view. The scenario lasts for 250 timesteps and two vessels spawn at the edge of the surveillance area every 20 timesteps and persists for up to 200 timesteps. The extent is modeled by a ship that is 6 meters long, 3 meters wide, and has a pointed bow where the full width is achieved 2 meters behind it. The measurements are generated by simulating a LiDAR with a simulated maximum range of 100 m, angular resolution 0.25° and a modeled radial accuracy of 0.1 m, measurements are only generated if they hit a simulated hull and only one measurement is generated per angle, which simulates occlusion. In addition, clutter is generated using a PPP with $\lambda_c = 20$ and a uniform spatial distribution. The results are averaged over 100 Monte Carlo simulation runs.

B. Parameters

The PMBM parameters are chosen as follows, probability of detection $P^D = 0.9$, probability of survival $P^S = 0.99$, and clutter rate $\lambda_c = 20$. The gating probability is set at $P_G = 0.99$, the pruning parameters are 0.01 for the existence probability, 0.01 for PPP mixture components, and 0.01 for multi-Bernoulli mixture components. Both target models use σ_c = 0.2 m as the noise parameter for the CV model and σ_r = 0.3 m for the measurement noise, the GP model uses $\sigma_\phi = 0.1$ as noise for the constant angular velocity model. Both target models use 20 for the length of the gamma prediction window.

[1]The implementation for the GGIW model was taken from github.com/yuhsuansia/Extended-target-PMBM-tracker and this implementation was modified for use with the GP model

For the GP target model, we use 9 test angles to parametrize the extent and the hyperparameters are σ_f = 0.5 m, σ_r = 0.5 m, σ_n = 0.001 m, $l = \pi/4$ and the forgetting factor $\alpha = 0.01$. The maximum amount of IEKF iterations is 50. For the GGIW target model, we use 200 for the extent prediction window. The birth spatial density is defined according to the method defined above with 36 components and a range of 105 m and a velocity magnitude of 2 m/s. The extent prior is roughly equivalent to the true extent for the GP model and for the GGIW model it models an ellipse with the same length and width defining the semi-axes, this is combined with the prior heading to calculate a prior value for the shape matrix X. The prior value of the gamma distribution is $\alpha_0 = 1000$ and $\beta_0 = 100$. The covariance of the Gaussians is inflated to ensure coverage of the whole circle, the positional component is 20 m, the velocity components are 3 m/s, and for the GP model the heading component is π and the angular velocity is $\pi/4$. In the case of the extent, for the GP model the prior is given by the covariance function.

C. Performance Evaluation

To compare the performance of the trackers, the GOSPA metric [22] is used to provide a single metric for the performance of a multi-target tracking algorithm by incorporating localization error, missed targets, and false targets into a single metric. However, due to the different state spaces of the different target models, the distance measure is only comparable between the shared states, the position, and the velocity. Therefore these states are used to calculate the localization error. The parameters for the GOSPA metric were cut off $c = 10$ and power $p = 2$. To compare the extent estimates of the target models we use the process of associating estimates to targets to generate additional measures that are comparable between them. One such measure is the Intersect-Over-Union (IOU) metric, which has been used in previous work to compare methods for extent estimation [11], [14]. To calculate the IOU metric for the GGIW model, the shape matrix X is decomposed to retrieve the length of the semi-axes, corresponding to the 2-σ ellipsoid, and the ellipse orientation. The heading error is calculated using the same method. Finally, the computation time for each run is also presented.

D. Results

The metrics are presented in Table I. Note the disparity of the IOU metric. This is primarily due to the inability of the GGIW model to model contour-generated measurements, since the GGIW model assumes a uniform distribution, and thus centers the ellipse on the contour instead, which causes large localization errors and large errors in extent estimation. Note also the larger heading error, showing an inability to estimate the heading as a separate state. The evolution of the metrics during the simulation run is shown in Fig 2. Here we can observe that the GGIW model exhibits track loss when the target ships pass the LiDAR and the origin points of the measurements change from the front to the stern or vice versa,

TABLE I
MEAN VALUE OF METRICS FOR THE SIMULATED SCENARIO

Model	GP	GGIW
GOSPA	**4.15**	7.54
Loc. Err.	**3.40**	6.45
Missed	**0.10**	0.57
False	**0.28**	0.45
IOU	**0.60**	0.22
Heading (rad)	**0.46**	1.62
Time (s)	63.71	**46.30**

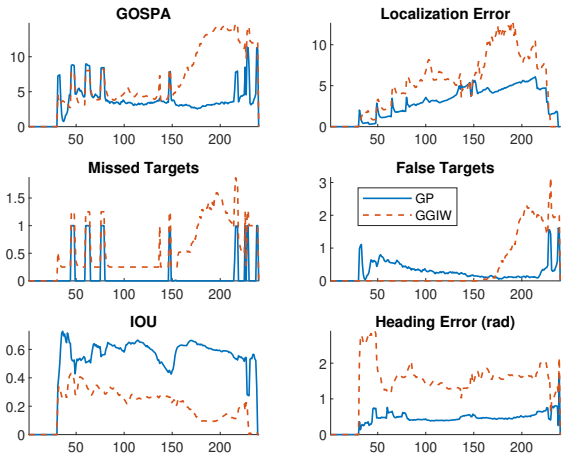

Fig. 2. The evolution over the course of the simulation run for selected metrics

which happens around timestep 170. The GP model is more computationally expensive, which is to be expected due to the use of GN optimization.

V. TEST DATA

In this section, we present the result from real LiDAR data gathered from tests in Trondheim utilizing the two platforms milliAmpere and milliAmpere2 in the Trondheim canal [23].

A. Test scenario

We present two separate scenarios, one with a single vessel performing maneuvers in front of the sensor in the canal

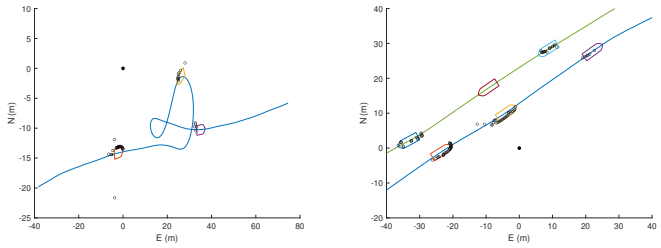

Fig. 3. Visualization of the test scenarios, along with the extent and measurements visualized for three different timesteps. Note measurements generated by the wake, as well as the occlusion in the second scenario.

(see Fig 3a) and one with two vessels traveling in separate directions in the canal and passing each other (see Fig 3b). The data from the first scenario was gathered using milliAmpere2 which is equipped with two Ouster OS1 32 LiDARs, these two point clouds were combined and the returns from land and static obstacles along the canal were filtered out using manual land masking and the point cloud was transformed to 2D by only retaining the point closest to the sensor in each angular resolution sector. The second scenario was published in [24] (as scenario 13) and is reused in this work. Note that for this scenario the ground truth data gathered was only positional GPS data without heading.

B. Parameters

Most of the parameters used are similar to the simulation study. The range used to define the birth density is reduced to 40 and 60 m respectively due to the observed range at which the LiDARs were able to detect the target vessels. For the second scenario, α_0 was set to 500 to account for the lower sensor resolution. The extent priors were set such that the length and width of the prior were roughly equivalent to the target vessels, but the same prior was used to represent both ships in the second scenario. In addition, some tweaks were made to attempt to mitigate some observed effects that are not modeled. To account for wake clutter, the clutter density was increased to $\lambda_c = 60$ and $\lambda_c = 100$ for the first and second scenario respectively, while the gating probability P_G was set to 0.95 for the same reason. Finally, to account for errors related to sway affecting the pitch of the LiDAR sensor, σ_r was set to 0.5.

C. Performance Evaluation

We use the same metrics that were used in the simulation study, with the ground truth data gathered used to calculate the metrics. For the first scenario, ground truth was measured by using a dual antenna INS system and the extent of the vessel was measured to be able to compare the estimated extent with the ground truth. For the second scenario, because only positional data was available, the heading was inferred from the velocity vector, which is a significant source of error for the calculation of the IOU and heading error metrics.

D. Results

The first scenario is quite simple from a target tracking perspective, it is simply a test of target birth and the ability of the target models to track the ship while it is performing complex maneuvers. The relevant metrics are presented in Table II, and the plots are shown in Fig. 4. The GP model is able to track the target over the whole scenario. However, as the target gets closer to the sensor the IOU measures degrade, this is due to wake clutter being detected by the LiDAR which is associated with the target, affecting the extent estimate. The estimate recovers when the vessel completes a turn. As the target vessel moves away, the track is lost, note also that as this happens the heading estimate flips to the reverse heading, which constitutes another local optimum of the cost function.

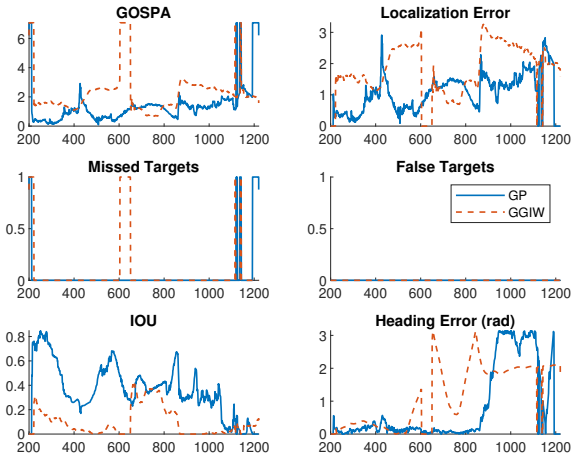

Fig. 4. The evolution over the course of the single target test run for selected metrics

TABLE II
MEAN VALUE OF METRICS FOR THE REAL LIDAR DATA

	Test 1		Test 2	
Model	GP	GGIW	GP	GGIW
GOSPA	**1.40**	2.32	5.69	**4.70**
Loc. Err.	**1.12**	1.94	6.02	**4.10**
Missed	**0.03**	0.05	**0.08**	0.12
False	**0.00**	0.00	0.02	**0.01**
IOU	**0.38**	0.10	0.18	**0.27**
Heading (rad)	**0.84**	1.26	**0.56**	2.25
Time (s)	112.06	**82.22**	474.04	**213.49**

The GGIW model is unable to maintain a track during the turning maneuver, but initiates a new track to continue tracking the target.

The second scenario is more complex, as it entails two targets, with one target being occluded by the other. The metrics are given in table II and the evolution over time is shown in Fig. 5. Here the GGIW model has a superior GOSPA score due to a lower localization error as well as a higher IOU. This is due to the disruptive effect of wake clutter on the GP model, which causes the extent estimates to get significantly worse when the wake is detectable, around timestep 1200, this also affects the centroid estimate, resulting in a larger localization error. The GGIW model does not suffer from the same shortcoming, due to the assumption that measurements are uniformly distributed.

VI. CONCLUSION

This paper has presented the use of the Gaussian Process model as a target model in the PMBM-tracker, presented an improvement of the GP target model by using Gauss-Newton optimization, and suggested a heuristic method to mitigate the fact that the measurement model is non-convex. We have also highlighted the need for a well-designed birth density and provided an example. More robust ways of solving these issues are an area of further research. Furthermore, we

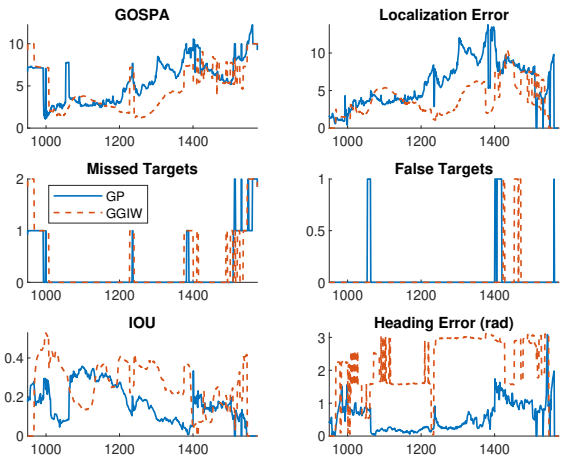

Fig. 5. The evolution over the course of the multi target test run for selected metrics

have demonstrated the resulting tracker on both simulated and real data and compared the performance against the standard GGIW-PMBM tracker. It shows that the GP model can generally track targets more accurately, as measured by GOSPA, and provide a better extent estimate when only a part of the target is detected by the sensor, as measured by the IOU metric. It also enables a correct heading estimate, since the heading is explicitly modeled as a part of the state, however local optima related to the heading is an issue that needs to be resolved. In addition, applying the method to real maritime data shows that wake clutter and occlusions are issues that need to be addressed. This is also an area that is of interest for further work.

Acknowledgment

The authors would like to acknowledge the help of Øystein Kaarstad Helgesen in providing data sets from milliAmpere, Erik Wilthil at Zeabuz and Egil Eide for assistance in collecting the data from milliAmpere2 and Simen Eldevik at DNV for providing ideas that contributed to the improvement of the Gauss-Newton optimization method used in the paper.

References

[1] K. Granstrom, M. Baum, and S. Reuter, "Extended Object Tracking: Introduction, Overview and Applications," *Journal of Advances in Information Fusion*, vol. 12, no. 2, pp. 139–174, Dec. 2017.

[2] J. W. Koch, "Bayesian approach to extended object and cluster tracking using random matrices," *IEEE Transactions on Aerospace and Electronic Systems*, vol. 44, no. 3, pp. 1042–1059, Jul. 2008.

[3] K. Granström, M. Fatemi, and L. Svensson, "Poisson Multi-Bernoulli Mixture Conjugate Prior for Multiple Extended Target Filtering," *IEEE Transactions on Aerospace and Electronic Systems*, vol. 56, no. 1, pp. 208–225, Feb. 2020.

[4] J. L. Williams, "Marginal multi-bernoulli filters: RFS derivation of MHT, JIPDA, and association-based member," *IEEE Transactions on Aerospace and Electronic Systems*, vol. 51, no. 3, pp. 1664–1687, Jul. 2015.

[5] K. Granström, S. Renter, M. Fatemi, and L. Svensson, "Pedestrian tracking using Velodyne data — Stochastic optimization for extended object tracking," in *2017 IEEE Intelligent Vehicles Symposium (IV)*, Jun. 2017, pp. 39–46.

[6] K. Granström, L. Svensson, S. Reuter, Y. Xia, and M. Fatemi, "Likelihood-Based Data Association for Extended Object Tracking Using Sampling Methods," *IEEE Transactions on Intelligent Vehicles*, vol. 3, no. 1, pp. 30–45, Mar. 2018, conference Name: IEEE Transactions on Intelligent Vehicles.

[7] Y. Xia, K. Granström, L. Svensson, M. Fatemi, A. F. García-Fernández, and J. L. Williams, "Poisson Multi-Bernoulli Approximations for Multiple Extended Object Filtering," *IEEE Transactions on Aerospace and Electronic Systems*, vol. 58, no. 2, pp. 890–906, Apr. 2022.

[8] Y. Xia, A. F. García-Fernández, F. Meyer, J. L. Williams, K. Granström, and L. Svensson, "Trajectory PMB Filters for Extended Object Tracking Using Belief Propagation," Jul. 2022, arXiv:2207.10164 [eess]. [Online]. Available: http://arxiv.org/abs/2207.10164

[9] Y. Xia, K. Granström, L. Svensson, A. F. García-Fernández, and J. L. Williams, "Extended target Poisson multi-Bernoulli mixture trackers based on sets of trajectories," in *2019 22th International Conference on Information Fusion (FUSION)*, Jul. 2019, pp. 1–8.

[10] M. Baum and U. D. Hanebeck, "Shape tracking of extended objects and group targets with star-convex RHMs," in *14th International Conference on Information Fusion*, Jul. 2011, pp. 1–8.

[11] N. Wahlstrom and E. Ozkan, "Extended Target Tracking Using Gaussian Processes," *IEEE Transactions on Signal Processing*, vol. 63, no. 16, pp. 4165–4178, Aug. 2015.

[12] T. Hirscher, A. Scheel, S. Reuter, and K. Dietmayer, "Multiple extended object tracking using Gaussian processes," in *2016 19th International Conference on Information Fusion (FUSION)*, Jul. 2016, pp. 868–875.

[13] Y. Xia, K. Granstrom, L. Svensson, and A. F. García-Fernández, "Performance evaluation of multi-bernoulli conjugate priors for multi-target filtering," in *2017 20th International Conference on Information Fusion (Fusion)*, Jul. 2017, pp. 1–8.

[14] M. Kumru, H. Köksal, and E. Özkan, "Variational Measurement Update for Extended Object Tracking Using Gaussian Processes," *IEEE Signal Processing Letters*, vol. 28, pp. 538–542, 2021.

[15] S. Lee and J. McBride, "Extended Object Tracking via Positive and Negative Information Fusion," *IEEE Transactions on Signal Processing*, vol. 67, no. 7, pp. 1812–1823, Apr. 2019.

[16] M. Michaelis, P. Berthold, T. Luettel, D. Meissner, and H.-J. Wuensche, "Extended Object Tracking with an Improved Measurement-to-Contour Association," in *2020 IEEE 23rd International Conference on Information Fusion (FUSION)*, Jul. 2020, pp. 1–6.

[17] C. E. Rasmussen and C. K. I. Williams, *Gaussian processes for machine learning*, ser. Adaptive computation and machine learning. Cambridge, Mass: MIT Press, 2006, oCLC: ocm61285753.

[18] M. E. Lopez, "Poisson multi-Bernoulli mixture filter for multiple extended object tracking of maritime vessels using Lidar and Gaussian processes," 2020, publisher: NTNU. [Online]. Available: https://ntnuopen.ntnu.no/ntnu-xmlui/handle/11250/2781005

[19] K. Granström and U. Orguner, "Estimation and maintenance of measurement rates for multiple extended target tracking," in *2012 15th International Conference on Information Fusion*, Jul. 2012, pp. 2170–2176.

[20] C. Lundquist, K. Granström, and U. Orguner, "An Extended Target CPHD Filter and a Gamma Gaussian Inverse Wishart Implementation," *IEEE Journal of Selected Topics in Signal Processing*, vol. 7, no. 3, pp. 472–483, Jun. 2013.

[21] B. Bell and F. Cathey, "The iterated Kalman filter update as a Gauss-Newton method," *IEEE Transactions on Automatic Control*, vol. 38, no. 2, pp. 294–297, Feb. 1993.

[22] A. S. Rahmathullah, A. F. García-Fernández, and L. Svensson, "Generalized optimal sub-pattern assignment metric," in *2017 20th International Conference on Information Fusion (Fusion)*, Jul. 2017, pp. 1–8.

[23] E. F. Brekke, E. Eide, B.-O. H. Eriksen, E. F. Wilthil, M. Breivik, E. Skjellaug, Ø. K. Helgesen, A. M. Lekkas, A. B. Martinsen, E. H. Thyri, T. Torben, E. Veitch, O. A. Alsos, and T. A. Johansen, "milliAmpere: An Autonomous Ferry Prototype," *Journal of Physics: Conference Series*, vol. 2311, no. 1, p. 012029, Jul. 2022, publisher: IOP Publishing.

[24] Ø. K. Helgesen, K. Vasstein, E. F. Brekke, and A. Stahl, "Heterogeneous multi-sensor tracking for an autonomous surface vehicle in a littoral environment," *Ocean Engineering*, vol. 252, p. 111168, May 2022.